中國科學院高能物理研究所
Institute of High Energy Physics, Chinese Academy of Sciences

NLO corrections to nucleon axial-vector form factors

An extension of the Dirac form factors work: *Phys.Rev.Lett.* 135 (2025) 13, 131903

Hard exclusive nucleon structure at large momentum transfer

Yang Liu – Institute of High Energy Physics, Chinese Academy of Sciences

In collaboration with Feng Feng, Yu Jia, Jichen Pan
Paper in preparation

Outline

- Background and motivation
- Calculation techniques
- Recap of the Dirac results
- Two-loop renormalization group evolution
- Preliminary axial results

Why form factors?

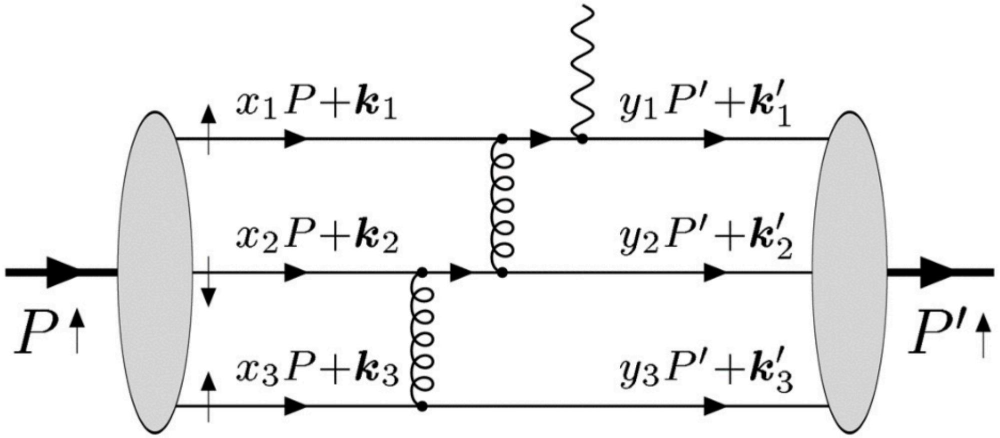

Electromagnetic current
Charge and magnetization distributions inside the nucleon.

$$\langle P' | j^{\mu}_{\mathrm{em}} | P \rangle = \bar{N}(P') \left[F_1(Q^2)\gamma^{\mu} - F_2(Q^2) \frac{i\sigma^{\mu\nu} q_{\nu}}{2m_N} \right] N(P)$$

Why form factors?

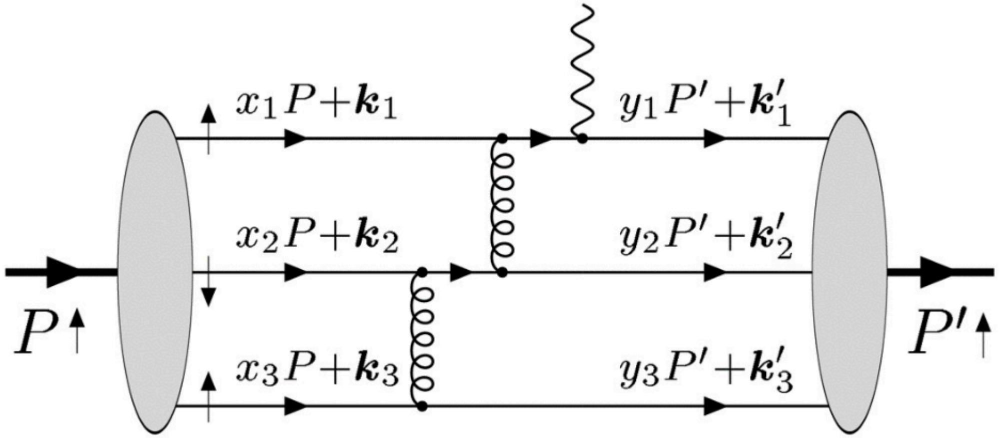

N. G. Stefanis and M. Bergmann *Phys.Rev.D* 47 (1993) R3685-R3689

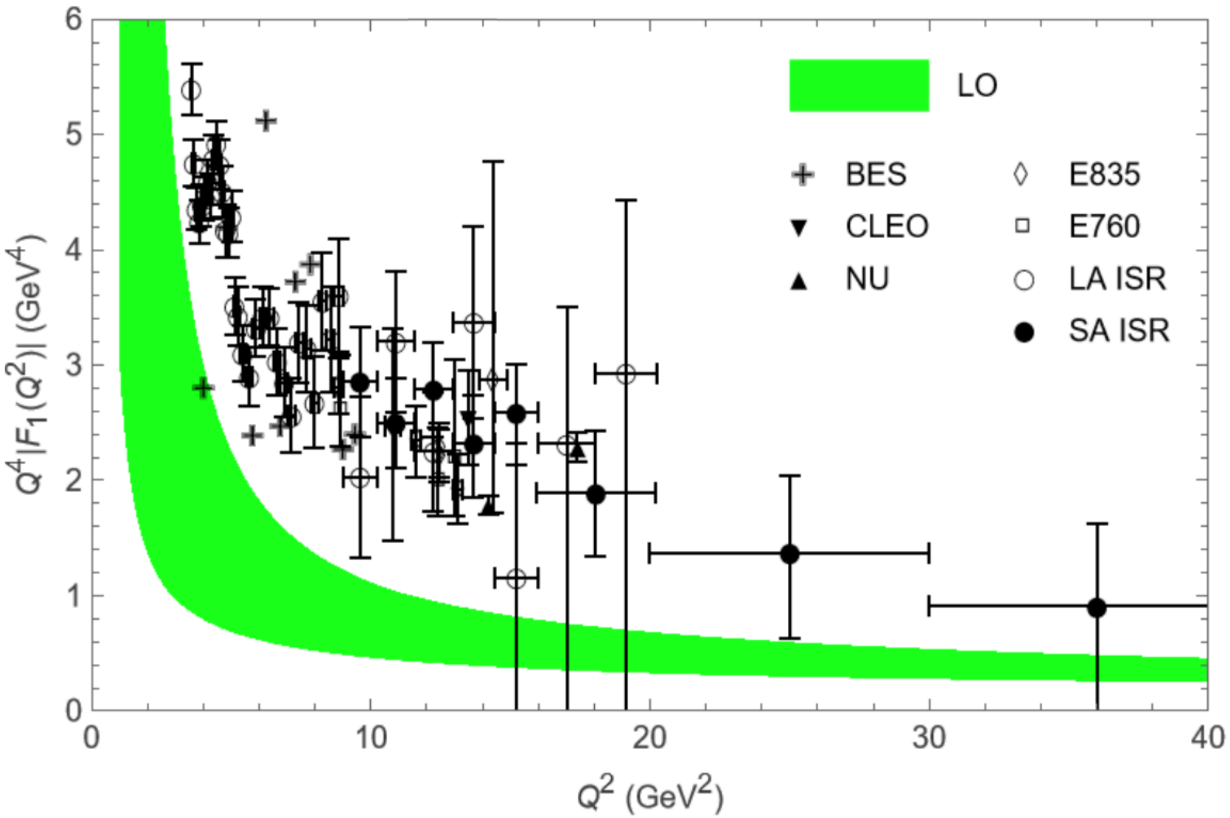

Electromagnetic current
Charge and magnetization distributions inside the nucleon.

$$\langle P'|j^\mu_{\text{em}}|P\rangle = \bar{N}(P')\left[F_1(Q^2)\gamma^\mu - F_2(Q^2)\frac{i\sigma^{\mu\nu}q_\nu}{2m_N}\right]N(P)$$

Axial current
Spin/isovector weak structure, essential for neutrino and β-decay physics.

$$\langle P'|A^\mu|P\rangle = \bar{N}(P')\left[G_A(Q^2)\gamma^\mu\gamma_5 + G_P(Q^2)\frac{q^\mu\gamma_5}{2m_N}\right]N(P)$$

Helicity-conserving form factors are studied most

$$\langle P'|j^\mu_{\text{em}}|P\rangle = \bar{N}(P')\left[F_1(Q^2)\gamma^\mu - F_2(Q^2)\frac{i\sigma^{\mu\nu}q_\nu}{2m_N}\right]N(P)$$

$$\langle P'|A^\mu|P\rangle = \bar{N}(P')\left[G_A(Q^2)\gamma^\mu\gamma_5 + G_P(Q^2)\frac{q^\mu\gamma_5}{2m_N}\right]N(P)$$

F_1

G_A

helicity conserving

~ $1 / Q^4$ asymptotically

Helicity-conserving form factors are studied most

$$\langle P'|j^\mu_{\mathrm{em}}|P\rangle = \bar{N}(P')\left[F_1(Q^2)\gamma^\mu - F_2(Q^2)\frac{i\sigma^{\mu\nu}q_\nu}{2m_N}\right]N(P)$$

$$\langle P'|A^\mu|P\rangle = \bar{N}(P')\left[G_A(Q^2)\gamma^\mu\gamma_5 + G_P(Q^2)\frac{q^\mu\gamma_5}{2m_N}\right]N(P)$$

F_1
G_A

helicity conserving
~ 1 / Q^4 asymptotically

F_2
G_P

helicity flipping
~ 1 / Q^6 asymptotically

Axial form factors help understand weak force

$$\langle P'|A^\mu|P\rangle = \bar{N}(P')\left[G_A(Q^2)\gamma^\mu\gamma_5 + G_P(Q^2)\frac{q^\mu\gamma_5}{2m_N}\right]N(P)$$

$$g_A = G_A(0) = \Delta u - \Delta d$$

- Connects low-energy weak decay with the spin-flavor structure of the nucleon
- Required in analyses of the neutron lifetime
- Can be used to test first-row CKM unitarity V_{ud}

Axial form factors help understand weak force

$$\langle P'|A^\mu|P\rangle = \bar{N}(P')\left[G_A(Q^2)\gamma^\mu\gamma_5 + G_P(Q^2)\frac{q^\mu\gamma_5}{2m_N}\right]N(P)$$

$$g_A = G_A(0) = \Delta u - \Delta d$$

- Connects low-energy weak decay with the spin-flavor structure of the nucleon
- Required in analyses of the neutron lifetime
- Can be used to test first-row CKM unitarity V_{ud}

$$\nu_\ell n \to \ell^- p$$

One of the dominant free-nucleon uncertainties in

- ❑ neutrino-energy reconstruction
- ❑ event classification in oscillation experiments
- ❑ extraction of neutrino mixing parameters and leptonic CP violation

Axial form factors help understand weak force

$$G_A^{\mathrm{dip}}(Q^2) = \frac{g_A}{\left(1 + Q^2/M_A^2\right)^2} \qquad g_A = 1.2723(23)$$ *Phys.Rev.D* 110 (2024) 3, 030001

Axial form factors help understand weak force

$$G_A^{\mathrm{dip}}(Q^2) = \frac{g_A}{(1 + Q^2/M_A^2)^2}$$

$g_A = 1.2723(23)$ *Phys.Rev.D* 110 (2024) 3, 030001

Leading-order calculations

S. J. Brodsky, G. P. Lepage and S. A. A. Zaidi
Phys.Rev.D 23 (1981) 1152

C. E. Carlson and J. L. Poor
Phys.Rev.D 34 (1986) 1478

Axial form factors help understand weak force

$$G_A^{\mathrm{dip}}(Q^2) = \frac{g_A}{(1+Q^2/M_A^2)^2}$$

$g_A = 1.2723(23)$ *Phys.Rev.D* 110 (2024) 3, 030001

Leading-order calculations

S. J. Brodsky, G. P. Lepage and S. A. A. Zaidi
Phys.Rev.D 23 (1981) 1152

C. E. Carlson and J. L. Poor
Phys.Rev.D 34 (1986) 1478

Further attempts

I. V. Anikin, V. M. Braun and N. Offen
Phys.Rev.D 94 (2016) 3, 034011

X. Y. Liu, A. Limphirat, K. Xu, Z. Zhao, K. Khosonthongkee and Y. Yan
Phys.Rev.D 107 (2023) 7, 074006

C. Chen and C. D. Roberts
Eur.Phys.J.A 58 (2022) 10, 206

NLO correction $\sim 40\%$ at $Q^2 \simeq 1$–$2\ \mathrm{GeV}^2$

Lattice QCD

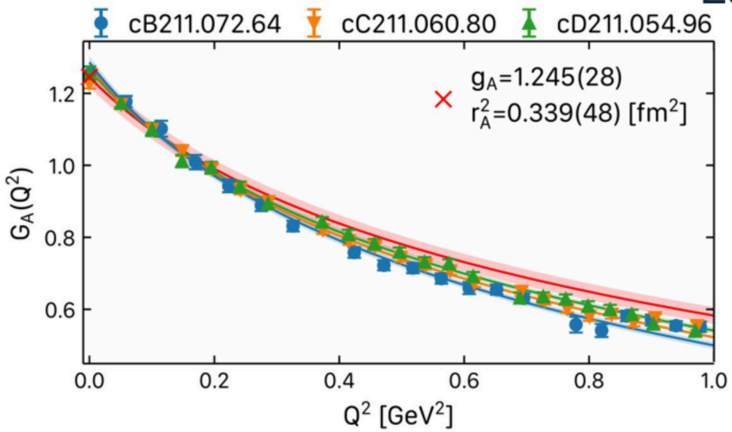

PoS LATTICE2024 (2025) 346

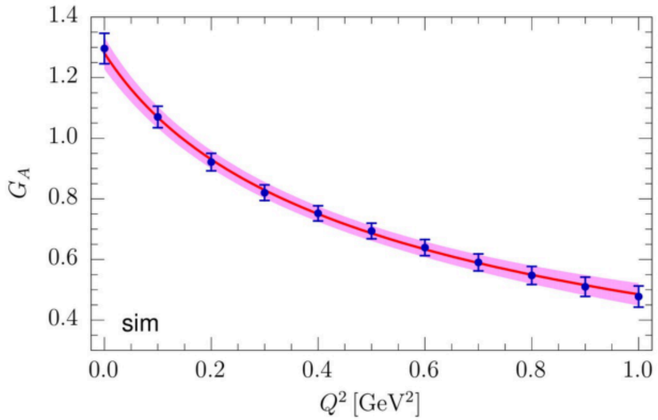

Phys.Rev.D 109 (2024) 1, 014503

A nearly 50-year gap bridged

1977–80

LO scattering kernel for nucleon F_1

2025

First complete NLO Dirac hard kernel

L. B. Chen, W. Chen, F. Feng, S. Hu and Y. Jia
Phys.Rev.Lett. 135 (2025) 13, 131903

Y. K. Huang, B. X. Shi, Y. M. Wang and X. C. Zhao
Phys.Rev.Lett. 135 (2025) 6, 061901

A nearly 50-year gap bridged

1977–80

LO scattering kernel for nucleon F_1

2025

First complete NLO Dirac hard kernel

L. B. Chen, W. Chen, F. Feng, S. Hu and Y. Jia
Phys.Rev.Lett. 135 (2025) 13, 131903

Y. K. Huang, B. X. Shi, Y. M. Wang and X. C. Zhao
Phys.Rev.Lett. 135 (2025) 6, 061901

2026

First two-loop nucleon-DA RGE

Y. K. Huang, Y. Ji, B. X. Shi and Y. M. Wang
2512.20471 [hep-ph]

A nearly 50-year gap bridged

1977–80

LO scattering kernel for nucleon F_1

2025

First complete NLO Dirac hard kernel

L. B. Chen, W. Chen, F. Feng, S. Hu and Y. Jia
Phys.Rev.Lett. 135 (2025) 13, 131903

Y. K. Huang, B. X. Shi, Y. M. Wang and X. C. Zhao
Phys.Rev.Lett. 135 (2025) 6, 061901

2026

First two-loop nucleon-DA RGE

Y. K. Huang, Y. Ji, B. X. Shi and Y. M. Wang
2512.20471 [hep-ph]

NLO is positive and substantial

Across different DA models and energy scales, the NLO hard contribution is positive and substantial.

But some gaps still exist

With modern lattice DAs, the leading-power hard contribution remains well below the measured data.

Collinear factorization separates the scales

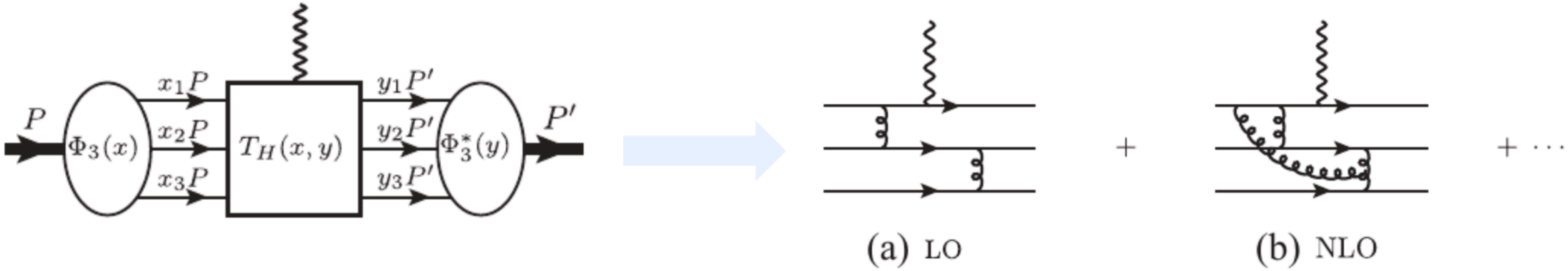

DA ⊗ hard kernel ⊗ DA

LO: α_s^2 | NLO: α_s^3

Collinear factorization separates the scales

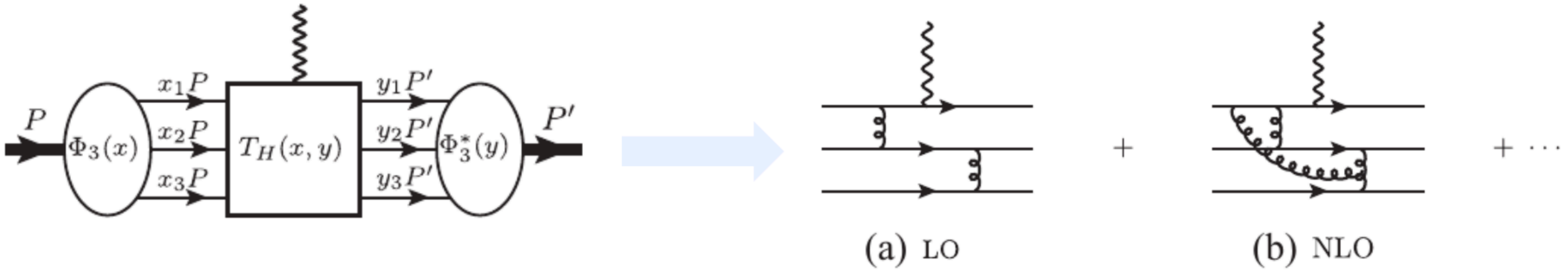

DA ⊗ hard kernel ⊗ DA

LO: α_s^2 | NLO: α_s^3

$$Q^4 F_1(Q^2) = \Phi_N^*(y,\mu_F) \underset{y}{\otimes} T_H(x,y,Q^2;\mu_R,\mu_F) \underset{x}{\otimes} \Phi_N(x,\mu_F) + \mathcal{O}\left(\frac{1}{Q^2}\right)$$

universal | process specific | universal

Two hard gluons distribute the large momentum among three valence quarks, so the form factor begins at α_s^2 / Q^4.

DA expanded in orthogonal polynomials

$$\Phi_N(x,\mu) = f_N(\mu)\,120 x_1 x_2 x_3 \sum_{M,m} \varphi_{Mm}(\mu)\,\mathcal{P}_{Mm}(x)$$

Normalization

$$f_N(\mu)$$

Sets the overall hard amplitude; the form factor scales with its square.

Shape moments

$$\varphi_{Mm}(\mu)$$

Encodes asymmetry and higher conformal waves; DA models diverge here.

DA expanded in orthogonal polynomials

$$\Phi_N(x,\mu) = f_N(\mu)\,120x_1x_2x_3 \sum_{M,m} \varphi_{Mm}(\mu)\,\mathcal{P}_{Mm}(x)$$

Normalization

$$f_N(\mu)$$

Sets the overall hard amplitude; the form factor scales with its square.

Shape moments

$$\varphi_{Mm}(\mu)$$

Encodes asymmetry and higher conformal waves; DA models diverge here.

Evolution

$$U(\mu,\mu_0)$$

Resums collinear logs and evolves the DA to other scales.

Scattering kernel oblivious of long distances

Substitute the free, collinear three-quark states for the complex nucleon states

$$|P_+\rangle^0_{1/2} \Rightarrow |\{p_i\}\rangle_{1/2} = \frac{1}{\sqrt{6}}\epsilon_{abc}u^\dagger_{a+}(p_1)\left[u^\dagger_{b-}(p_2)d^\dagger_{c+}(p_3) - d^\dagger_{b-}(p_2)u^\dagger_{c+}(p_3)\right]|0\rangle = |uud,\{p_i\}\rangle - |udu,\{p_i\}\rangle$$

Scattering kernel oblivious of long distances

Substitute the free, collinear three-quark states for the complex nucleon states

$$|P_+\rangle^0_{1/2} \Rightarrow |\{p_i\}\rangle_{1/2} = \frac{1}{\sqrt{6}}\epsilon_{abc}u^\dagger_{a+}(p_1)\left[u^\dagger_{b-}(p_2)d^\dagger_{c+}(p_3) - d^\dagger_{b-}(p_2)u^\dagger_{c+}(p_3)\right]|0\rangle = |uud,\{p_i\}\rangle - |udu,\{p_i\}\rangle$$

Use antisymmetric Dirac basis

$$\mathcal{Q}^{abc}_{\alpha\beta\gamma} = \epsilon^{ijk}\, q^{ia}_\alpha\, q^{jb}_\beta\, q^{kc}_\gamma$$

$$\langle P'|j^\mu|P\rangle = \langle P'|[\bar{\mathcal{Q}}_{\alpha\beta\gamma}(y)]|0\rangle \underset{y}{\otimes} \mathcal{T}_{\alpha\beta\gamma;\alpha'\beta'\gamma'}(x,y) \underset{x}{\otimes} \langle 0|[\mathcal{Q}_{\alpha'\beta'\gamma'}(x)]|P\rangle$$

$$\mathcal{T}_{\alpha\beta\gamma;\alpha'\beta'\gamma'}(x,y) = T_{lmn}(x,y)\gamma^{(l)}_{\alpha\alpha'} \otimes \gamma^{(m)}_{\beta\beta'} \otimes \gamma^{(n)}_{\gamma\gamma'} \qquad \gamma^{(n)} = \gamma^{[\mu_1}\gamma^{\mu_2}\ldots\gamma^{\mu_n]}$$

Evanescent operators leave finite remnants

M. J. Dugan and B. Grinstein
Phys.Lett.B 256 (1991) 239-244

$$\mathcal{Q}^{abc}_{\alpha\beta\gamma} = \epsilon^{ijk} q^{ia}_{\alpha}\, q^{jb}_{\beta}\, q^{kc}_{\gamma}$$

d = 4 - 2ε → **physical + evanescent operators mix**

Evanescent operators leave finite remnants

M. J. Dugan and B. Grinstein
Phys.Lett.B 256 (1991) 239-244

$$\mathcal{Q}^{abc}_{\alpha\beta\gamma} = \epsilon^{ijk}\, q^{ia}_{\alpha}\, q^{jb}_{\beta}\, q^{kc}_{\gamma}$$

d = 4 - 2ε → **physical + evanescent operators mix**

O(ε) x 1 / ε = finite

Four-dimensional Fierz identities cannot be imposed on bare d-dimensional operators. $\langle 0|\mathcal{Q}_{\alpha\beta\gamma}(x)|P\rangle = \frac{1}{4}\left[\mathcal{V}(\boldsymbol{P}C)_{\alpha\beta}(\gamma^5 N)_\gamma + \mathcal{A}(\boldsymbol{P}\gamma^5 C)_{\alpha\beta}N_\gamma + \mathcal{T}(\mathrm{i}\sigma_{\mu\nu}P^\nu C)_{\alpha\beta}(\gamma^\mu\gamma^5 N)_\gamma\right]$

Evanescent contributions can be removed by finite renormalization.

Kränkl and Manashov's clever trick

S. Krankl and A. Manashov
Phys.Lett.B 703 (2011) 519-523

1

Keep spinor indices open

$$\mathcal{Q}^{abc}_{\alpha\beta\gamma} = \epsilon^{ijk} q^{ia}_{\alpha}\, q^{jb}_{\beta}\, q^{kc}_{\gamma}$$

2

Renormalize the open-index operator in d dimensions

$$[Q_{\alpha\beta\gamma}(x)]_{\mathrm{MS}} = Z^{\alpha'\beta'\gamma'}_{\alpha\beta\gamma}(x,x') \underset{x'}{\otimes} Q_{\alpha'\beta'\gamma'}(x')$$

Kränkl and Manashov's clever trick

S. Krankl and A. Manashov
Phys.Lett.B 703 (2011) 519-523

1

Keep spinor indices open

$$\mathcal{Q}^{abc}_{\alpha\beta\gamma} = \epsilon^{ijk} q^{ia}_{\alpha}\, q^{jb}_{\beta}\, q^{kc}_{\gamma}$$

2

Renormalize the open-index operator in d dimensions

$$[Q_{\alpha\beta\gamma}(x)]_{\mathrm{MS}} = Z^{\alpha'\beta'\gamma'}_{\alpha\beta\gamma}(x,x') \underset{x'}{\otimes} Q_{\alpha'\beta'\gamma'}(x')$$

3

Do the Dirac algebra

$$\mathcal{T}_{\alpha\beta\gamma;\alpha'\beta'\gamma'} = \sum_{lmn} T_{lmn}\, \gamma^{(l)}_{\alpha\alpha'} \otimes \gamma^{(m)}_{\beta\beta'} \otimes \gamma^{(n)}_{\gamma\gamma'}$$

$$\mathcal{A}_{\mathrm{phys}} = \bar{Z} \underset{y}{\otimes} T \underset{x}{\otimes} Z$$

- Evanescent operators vanish in 4d.
- Quark flavor structure is irrelevant in determining the renormalization factors.
- Renormalized Fierz identities are preserved.

The one-loop factorization checks out

48
tree diagrams

2040
one-loop diagrams

~100
master integrals

2
independent evaluation routes

The one-loop factorization checks out

48 tree diagrams

2040 one-loop diagrams

~100 master integrals

2 independent evaluation routes

- ✓ LO recovered
- ✓ UV poles removed by renormalization
- ✓ IR poles cancel pointwise by matching
- ✓ analytic ↔ 100-digit numerical check

Tools:
- HepLib: *Comput.Phys.Commun.* 285 (2023) 108631
- Apart: *Comput.Phys.Commun.* 183 (2012) 2158-2164
- FIRE: *Comput.Phys.Commun.* 302 (2024) 109261
- PolyLogTools: *JHEP* 08 (2019) 135

The one-loop factorization checks out

48	**2040**	**~100**	**2**
tree diagrams	one-loop diagrams	master integrals	independent evaluation routes

- ✓ LO recovered
- ✓ UV poles removed by renormalization
- ✓ IR poles cancel pointwise by matching
- ✓ analytic ↔ 100-digit numerical check

Tools:
HepLib: *Comput.Phys.Commun.* 285 (2023) 108631
Apart: *Comput.Phys.Commun.* 183 (2012) 2158-2164
FIRE: *Comput.Phys.Commun.* 302 (2024) 109261
PolyLogTools: *JHEP* 08 (2019) 135

Result: a pointwise IR-finite analytical hard kernel

One formula organizes scales and models

$$Q^4 F_1(Q^2) = f_N^2(\mu) \sum_{ijkl} \varphi_{ij}(\mu) H^{ijkl} \varphi^*_{kl}(\mu)$$

$$H^{ijkl} = \frac{1600\pi^2\alpha_s^2}{3} \left\{ Q_u c_0^{ijkl} \left[1 + \frac{\alpha_s}{\pi} \left(c_1^{ijkl} L_\mu + c_2^{ijkl} \right) \right] + Q_d d_0^{ijkl} \left[1 + \frac{\alpha_s}{\pi} \left(d_1^{ijkl} L_\mu + d_2^{ijkl} \right) \right] \right\}$$

One formula organizes scales and models

$$Q^4 F_1(Q^2) = f_N^2(\mu) \sum_{ijkl} \varphi_{ij}(\mu) H^{ijkl} \varphi_{kl}^*(\mu)$$

$$H^{ijkl} = \frac{1600\pi^2\alpha_s^2}{3} \left\{ Q_u c_0^{ijkl} \left[1 + \frac{\alpha_s}{\pi} \left(c_1^{ijkl} L_\mu + c_2^{ijkl} \right) \right] + Q_d d_0^{ijkl} \left[1 + \frac{\alpha_s}{\pi} \left(d_1^{ijkl} L_\mu + d_2^{ijkl} \right) \right] \right\}$$

$$L_\mu = \ln(\mu^2/Q^2)$$

neutron exchange up- and down-quark charges

timelike $L_\mu \to L_\mu + i\pi$

NLO corrections are positive and significant

Proton Spacelike

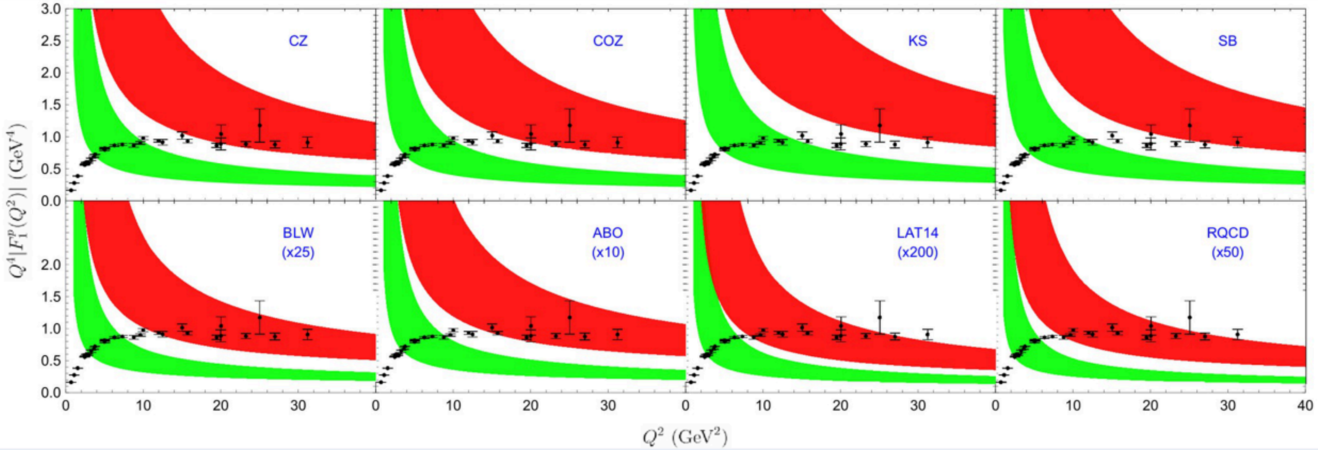

Proton Timelike

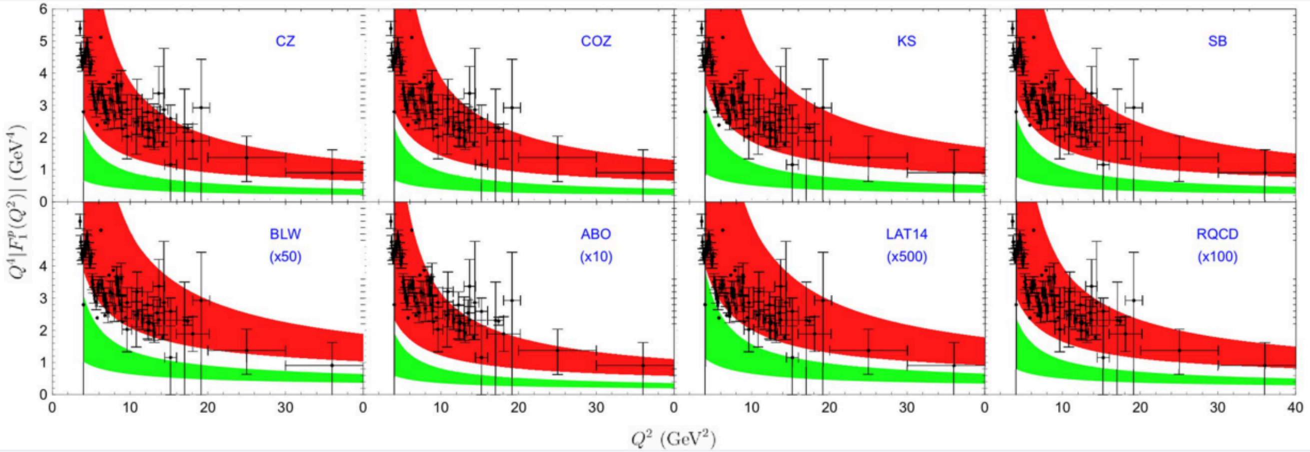

$$f_N(\mu) = f_N(\mu_0)\left(\frac{\alpha_s(\mu)}{\alpha_s(\mu_0)}\right)^{2/(3\beta_0)} \qquad \varphi_{mn}(\mu) = \varphi_{mn}(\mu_0)\left(\frac{\alpha_s(\mu)}{\alpha_s(\mu_0)}\right)^{\gamma_{mn}/\beta_0}$$

NLO corrections are positive and significant

Proton Spacelike

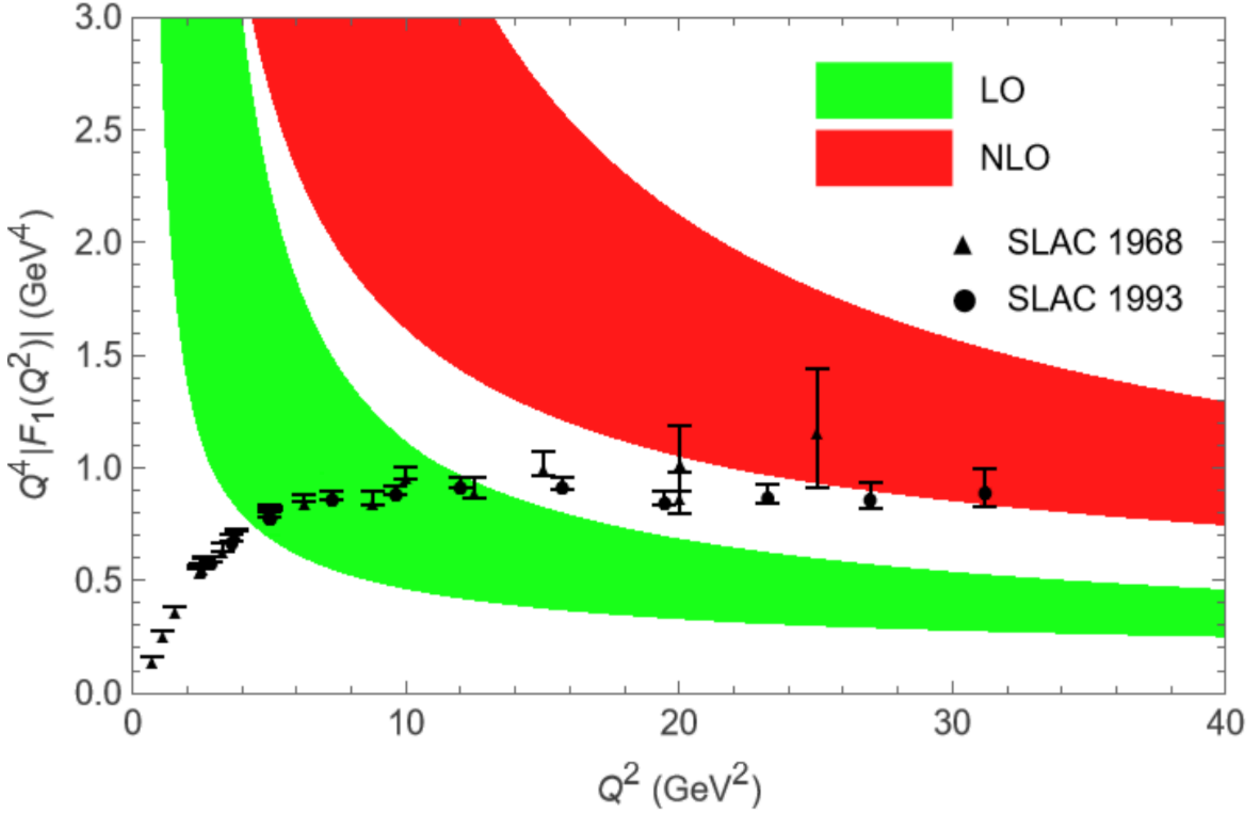

Proton Timelike

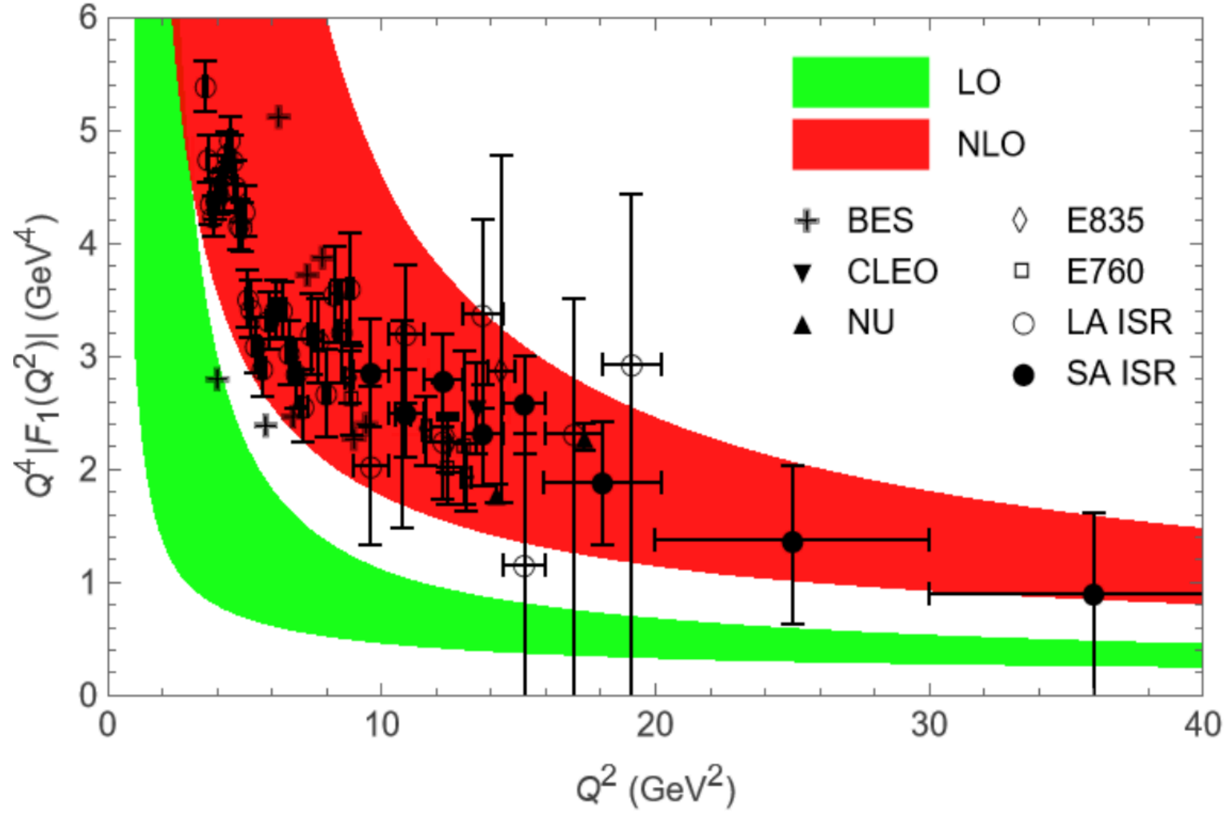

$$f_N(\mu) = f_N(\mu_0)\left(\frac{\alpha_s(\mu)}{\alpha_s(\mu_0)}\right)^{2/(3\beta_0)} \qquad \varphi_{mn}(\mu) = \varphi_{mn}(\mu_0)\left(\frac{\alpha_s(\mu)}{\alpha_s(\mu_0)}\right)^{\gamma_{mn}/\beta_0}$$

NLO corrections are positive and significant

Proton Spacelike

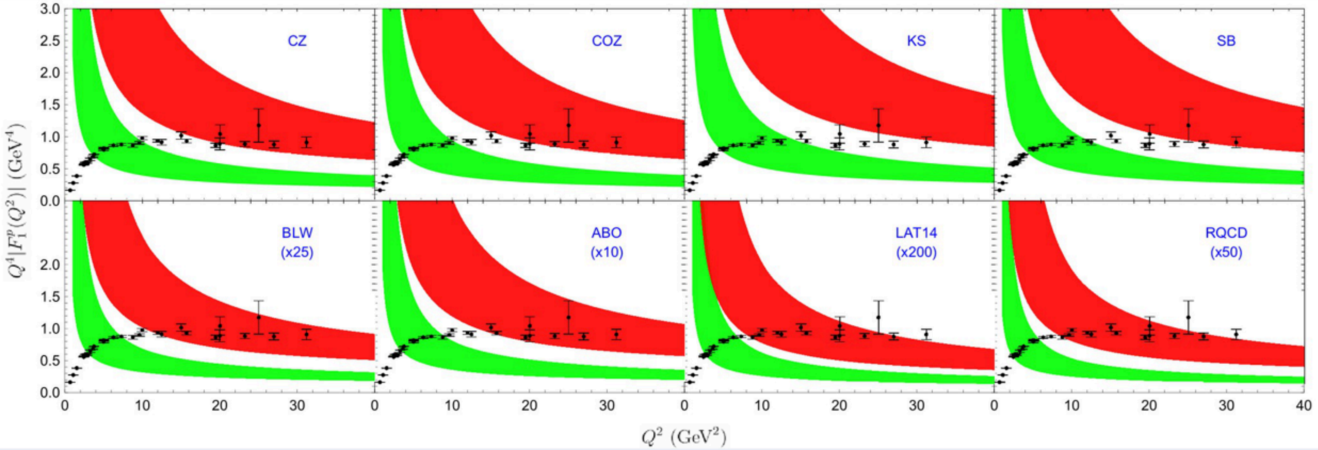

Proton Timelike

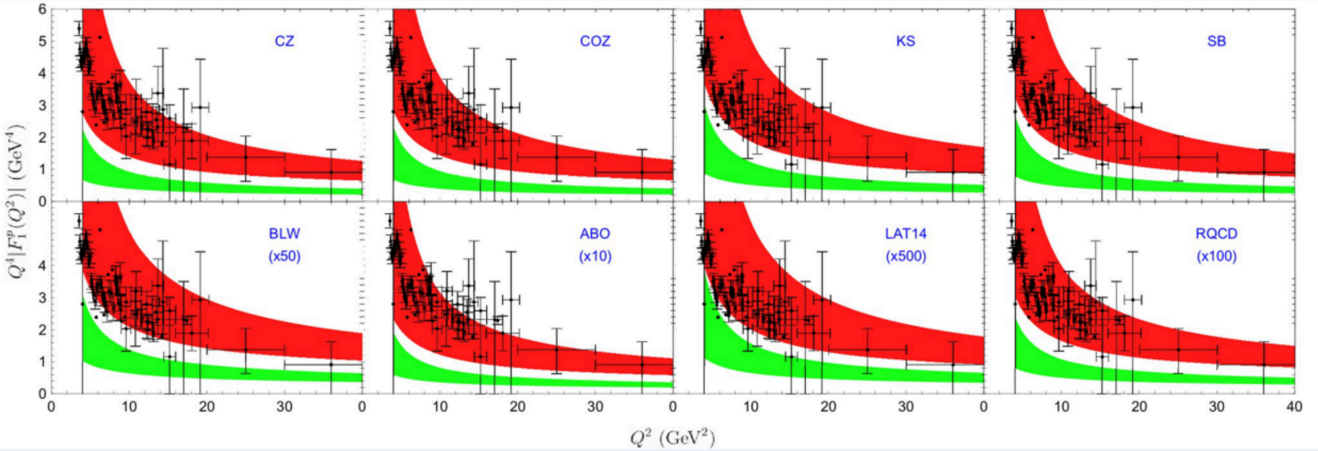

NLO significance

The one-loop hard kernel raises the pQCD prediction and reduces the historical LO underestimation.

Model sensitivity

QCD sum-rule LCDAs can reach the magnitude of large-Q^2 data, while small-coefficient lattice LCDAs are extremely low.

Important caveat

The predicted Q^2 trend is decreasing, whereas spacelike proton data show a flatter or rising pattern at large Q^2.

$$f_N(\mu) = f_N(\mu_0)\left(\frac{\alpha_s(\mu)}{\alpha_s(\mu_0)}\right)^{2/(3\beta_0)} \qquad \varphi_{mn}(\mu) = \varphi_{mn}(\mu_0)\left(\frac{\alpha_s(\mu)}{\alpha_s(\mu_0)}\right)^{\gamma_{mn}/\beta_0}$$

NLL evolution shifts normalized DA moments

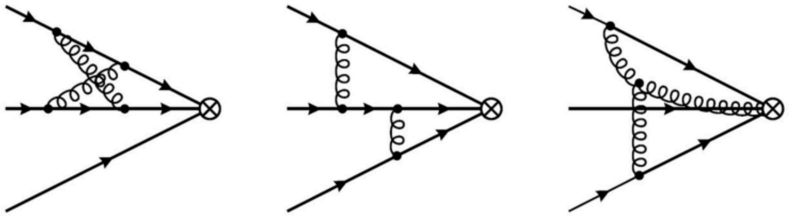

$$\boldsymbol{\Psi}(\mu) = \boldsymbol{U}_{\mathrm{NLL}}(\mu, \mu_0)\, \boldsymbol{\Psi}(\mu_0)$$

$$\mathbb{U}^{\mathrm{NLL}}(\mu,\, \mu_0) \;=\; \left(\mathbb{I} - \frac{\alpha_s(\mu)}{4\,\pi}\mathbb{J}^{(1)}\right) \left[\left(\frac{\alpha_s(\mu)}{\alpha_s(\mu_0)}\right)^{\frac{\mathbb{\Gamma}^{(0)}}{2\,\beta_0}}\right] \times \left(\mathbb{I} + \frac{\alpha_s(\mu_0)}{4\,\pi}\,\mathbb{J}^{(1)}\right)$$

Y. K. Huang, Y. Ji, B. X. Shi and Y. M. Wang
2512.20471 [hep-ph]

NLL evolution shifts normalized DA moments

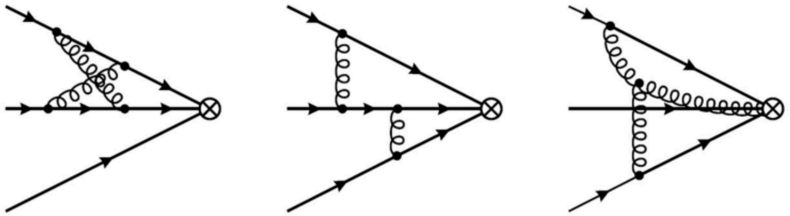

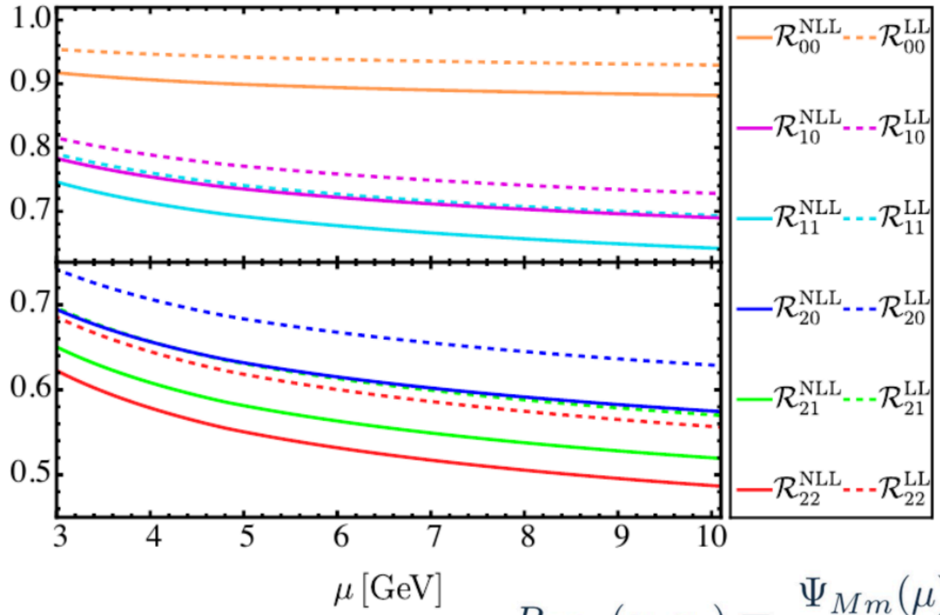

$$R_{Mm}(\mu, \mu_0) \equiv \frac{\Psi_{Mm}(\mu)}{\Psi_{Mm}(\mu_0)}$$

Solid: NLL   Dotted: LL

$$\boldsymbol{\Psi}(\mu) = \boldsymbol{U}_{\mathrm{NLL}}(\mu, \mu_0)\, \boldsymbol{\Psi}(\mu_0)$$

$$\mathbb{U}^{\mathrm{NLL}}(\mu,\, \mu_0) \;=\; \left(\mathbb{I} - \frac{\alpha_s(\mu)}{4\,\pi}\mathbb{J}^{(1)}\right) \left[\left(\frac{\alpha_s(\mu)}{\alpha_s(\mu_0)}\right)^{\frac{\Gamma^{(0)}}{2\,\beta_0}}\right] \times \left(\mathbb{I} + \frac{\alpha_s(\mu_0)}{4\,\pi}\,\mathbb{J}^{(1)}\right)$$

Y. K. Huang, Y. Ji, B. X. Shi and Y. M. Wang
2512.20471 [hep-ph]

NLL evolution shifts normalized DA moments

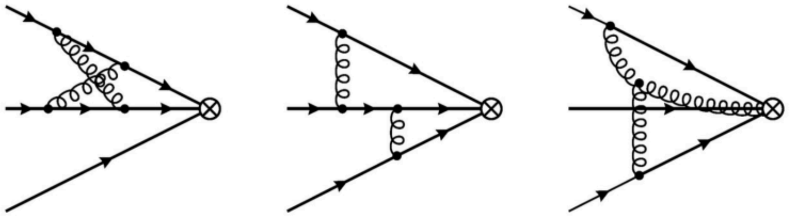

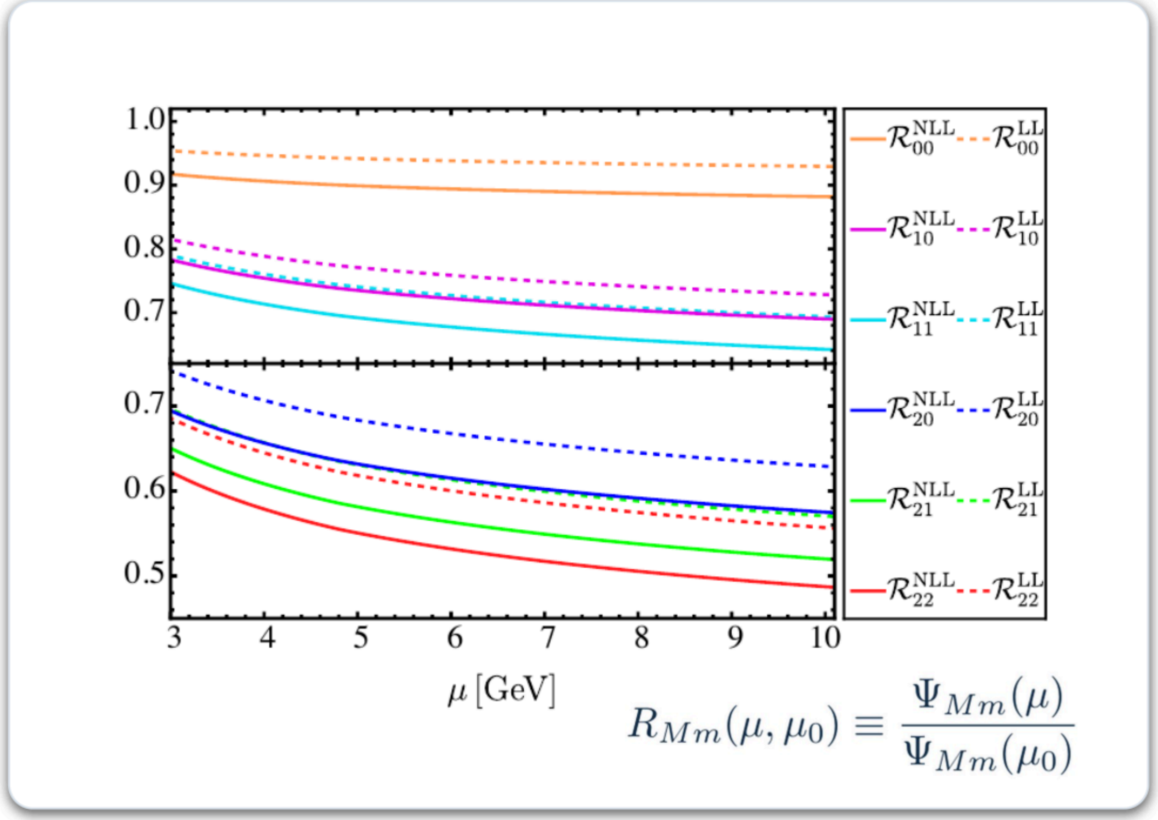

Solid: NLL   Dotted: LL

$$\boldsymbol{\Psi}(\mu) = \boldsymbol{U}_{\rm NLL}(\mu,\mu_0)\,\boldsymbol{\Psi}(\mu_0)$$

$$\mathbb{U}^{\rm NLL}(\mu,\,\mu_0) = \left(\mathbb{I} - \frac{\alpha_s(\mu)}{4\,\pi}\mathbb{J}^{(1)}\right)\left[\left(\frac{\alpha_s(\mu)}{\alpha_s(\mu_0)}\right)^{\frac{\Gamma^{(0)}}{2\,\beta_0}}\right] \times \left(\mathbb{I} + \frac{\alpha_s(\mu_0)}{4\,\pi}\,\mathbb{J}^{(1)}\right)$$

The solid NLL curves differ from dotted LL by up to ~20%; the shift is model-, scale-, and moment-dependent.

Higher-conformal-spin moments receive the larger corrections.

This universal input propagates into leading-twist hard Dirac and axial form factors.

Y. K. Huang, Y. Ji, B. X. Shi and Y. M. Wang
2512.20471 [hep-ph]

Scheme consistency constrains both DA legs

incoming DA

at μ_0 · EO/KM tagged

outgoing DA

at μ_0 · EO/KM tagged

Finite EO → KM conversion plus NLL evolution

$$U_{\mathrm{KM}}(\mu,\mu_0) = C(\mu)\,U_{\mathrm{EO}}(\mu,\mu_0)\,C^{-1}(\mu_0)$$

apply separately to each external DA leg

incoming DA

at μ · selected scheme

outgoing DA

at μ · selected scheme

Scheme consistency constrains both DA legs

incoming DA
at μ_0 · EO/KM tagged

outgoing DA
at μ_0 · EO/KM tagged

Finite EO → KM conversion plus NLL evolution

$$U_{\mathrm{KM}}(\mu,\mu_0) = C(\mu)\, U_{\mathrm{EO}}(\mu,\mu_0)\, C^{-1}(\mu_0)$$

apply separately to each external DA leg

incoming DA
at μ · selected scheme

outgoing DA
at μ · selected scheme

The scattering kernel transforms in the same way

$$H_{\mathrm{KM}} = C\, H_{\mathrm{EO}}\, C^{-1}$$

The results are scheme independent when both DAs and the kernel are converted consistently.

The axial channel reuses the precision chain

$$\langle P'|A^{\mu}|P\rangle = \bar{N}(P')\left[G_A(Q^2)\gamma^{\mu}\gamma_5 + G_P(Q^2)\frac{q^{\mu}\gamma_5}{2m_N}\right]N(P)$$

Inherits from Dirac

- twist-3 nucleon LCDA basis
- KM renormalization infrastructure
- convolution and uncertainty machinery

The axial channel reuses the precision chain

$$\langle P'|A^\mu|P\rangle = \bar{N}(P')\left[G_A(Q^2)\gamma^\mu\gamma_5 + G_P(Q^2)\frac{q^\mu\gamma_5}{2m_N}\right]N(P)$$

Inherits from Dirac

- twist-3 nucleon LCDA basis
- KM renormalization infrastructure
- convolution and uncertainty machinery

$$|N_+\rangle^0_{1/2} \Rightarrow |\{p_i\}\rangle_{1/2} = \frac{1}{\sqrt{6}}\epsilon_{abc}d^\dagger_{a+}(p_1)\left[u^\dagger_{b-}(p_2)d^\dagger_{c+}(p_3) - d^\dagger_{b-}(p_2)u^\dagger_{c+}(p_3)\right]|0\rangle = |dud,\{p_i\}\rangle - |ddu,\{p_i\}\rangle$$

$$\begin{aligned}\langle\{p'_i\}|_{1/2}\,\bar{d}\gamma^\mu\gamma^5 u\,|\{p_i\}\rangle_{1/2} = {} & \langle dud,\{p'_i\}|\,\bar{d}\gamma^\mu\gamma^5 u\,|uud,\{p_i\}\rangle - \langle ddu,\{p'_i\}|\,\bar{d}\gamma^\mu\gamma^5 u\,|uud,\{p_i\}\rangle \\ & + \langle ddu,\{p'_i\}|\,\bar{d}\gamma^\mu\gamma^5 u\,|udu,\{p_i\}\rangle\end{aligned}$$

Complete NLL axial prediction = two-loop DA evolution + NLO axial kernel + consistent EO/KM conversion on both legs + declared flavor current and γ5 scheme.

Preliminary results are similar

$$H^{ijkl} = -\frac{1600\pi^2\alpha_s^2}{3} c_0^{ijkl}\left[1 + \frac{\alpha_s}{\pi}\left(c_1^{ijkl} L_\mu + c_2^{ijkl}\right)\right]$$

Spacelike

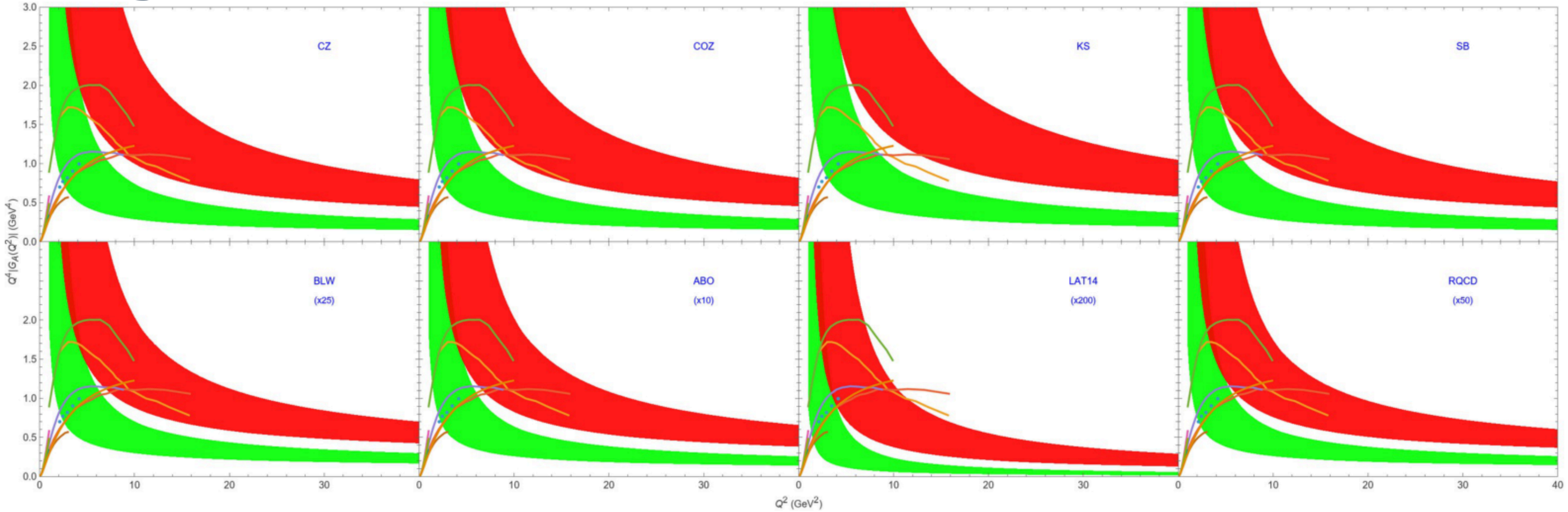

Timelike

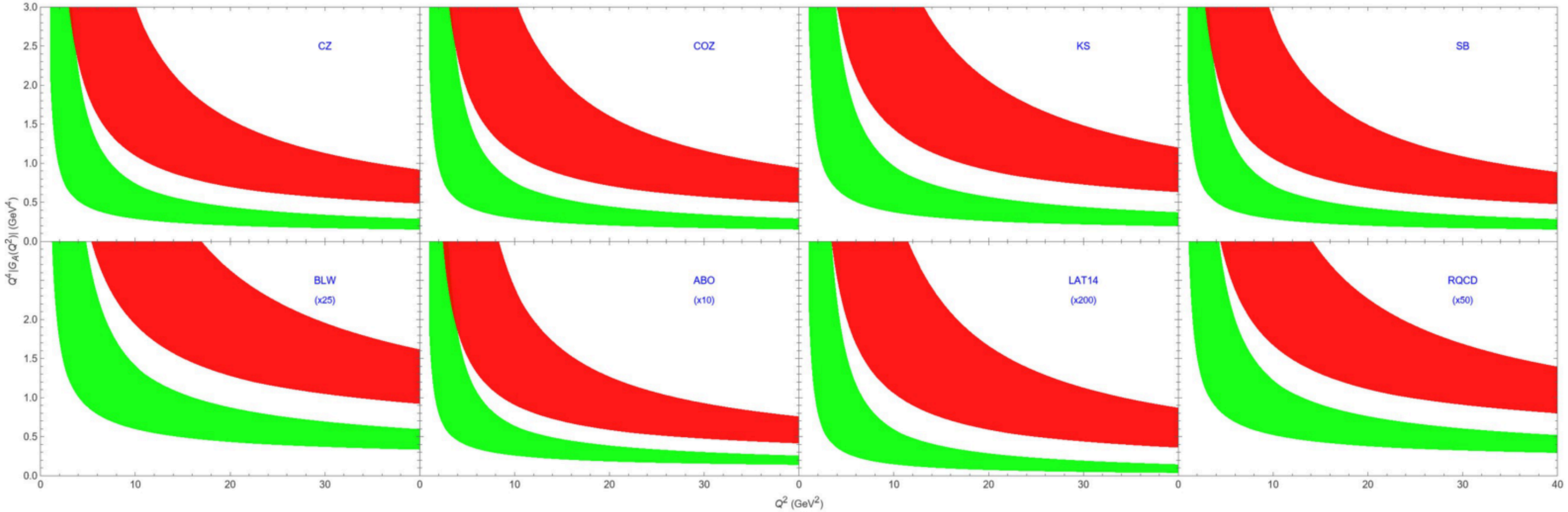

Preliminary results are similar

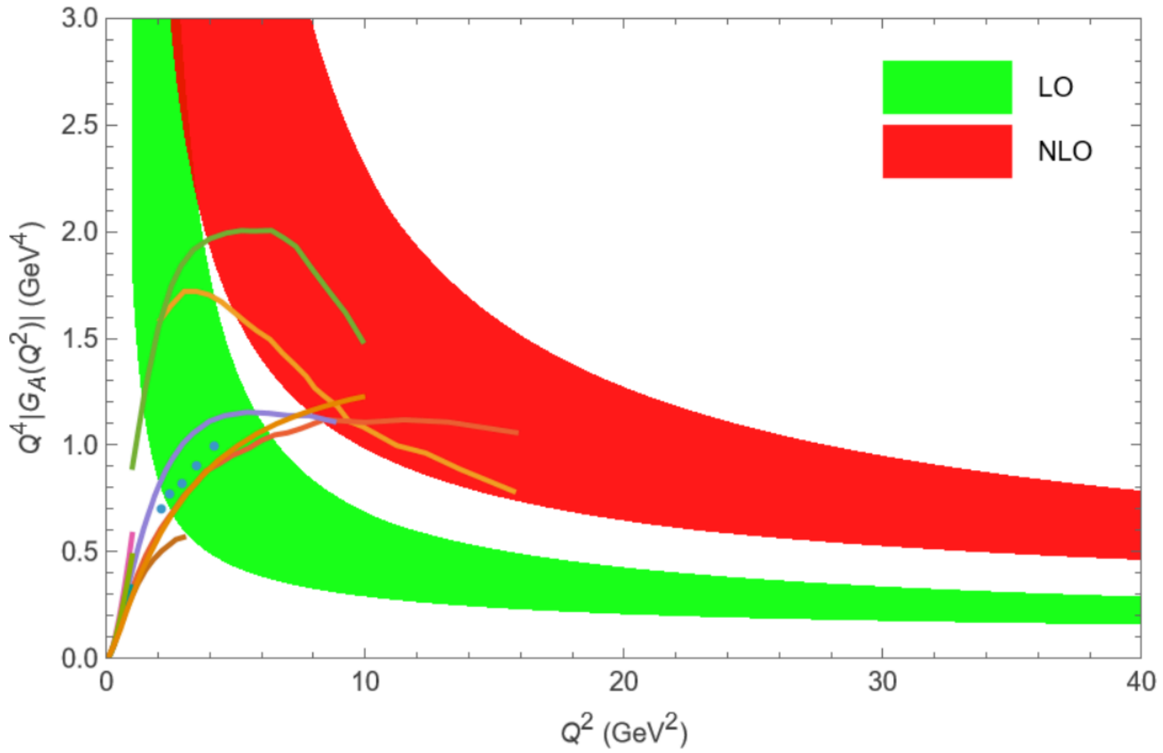

NLO remains essential

The positive NLO effect is still visible, and shows some agreement with other models.

Preliminary results are similar

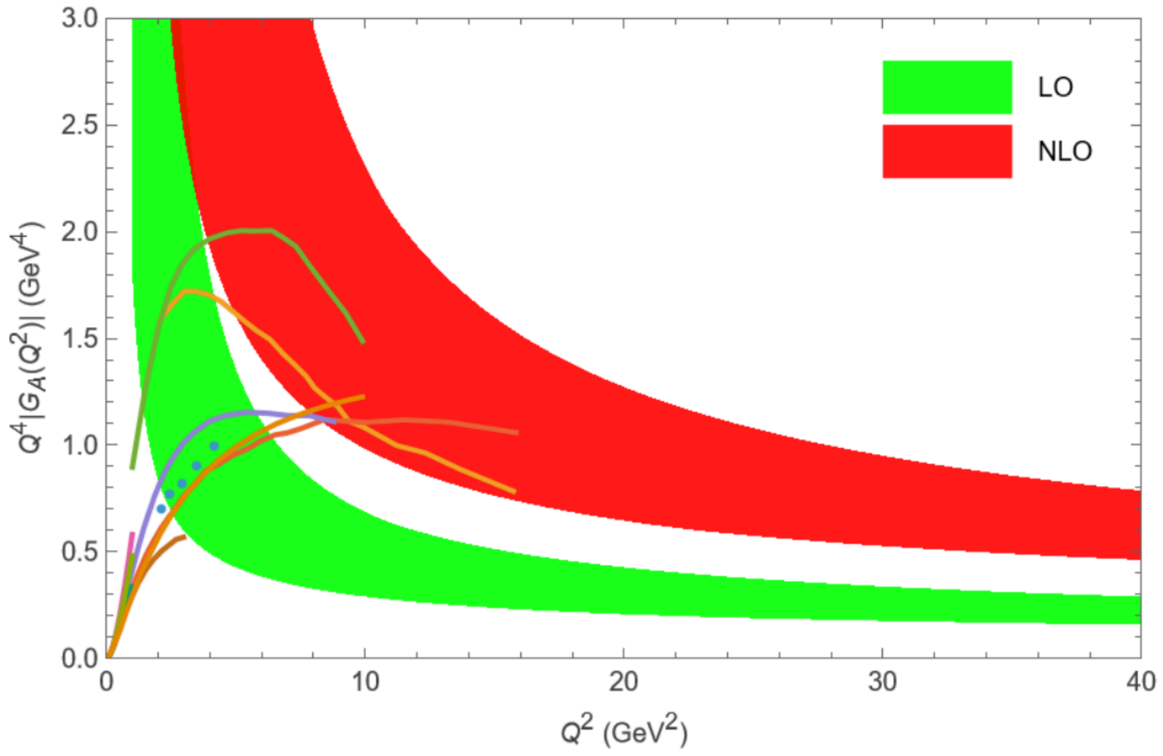

NLO remains essential

The positive NLO effect is still visible, and shows some agreement with other models.

Data limitations

Available data are way less extensive than Dirac data, so the phenomenological discrimination is weaker.

Model sensitivity

Lattice-DA predictions are extremely low in the axial case too.

The precision picture is clear yet incomplete

1. Following up the first ever results of NLO corrections to the nucleon Dirac form factors in nearly half a century, using the collinear factorization theorem in the KM renormalization scheme.

2. Two-loop evolution completes universal NLL DA running, and axial-vector results are underway.

3. NLO substantially raises the predictions, yet lattice-DA predictions remain far below. Large-momentum effective theory? Failure of factorization?

CONCLUSION

The precision picture is clear yet incomplete

1. Following up the first ever results of NLO corrections to the nucleon Dirac form factors in nearly half a century, using the collinear factorization theorem in the KM renormalization scheme.
2. Two-loop evolution completes universal NLL DA running, and axial-vector results are underway.
3. NLO substantially raises the predictions, yet lattice-DA predictions remain far below. Large-momentum effective theory? Failure of factorization?

Longbin Chen, Wen Chen, Feng Feng, Siwei Hu, Yu Jia, Jichen Pan

Thanks!

Questions and comments are welcome.